MEDDOCS Open Access Publisher

ISSN: 2639-4383

Annals of Cardiology and Vascular Medicine

Open Access | Research Article

Longitudinal Evaluation of Aortic Haemodynamics in Patients after Repair of Aortic Coarctation: A 4D Flow MRI Follow-Up Study

Daniel Hirtler[1]; Julia Romberg[2]; Brigitte Stiller[1]; Julia Geiger[3,4,5]

[1]Department of Congenital Heart Disease and Paediatric Cardiology, University Heart Centre. Freiburg, Bad Krozingen, University of Freiburg, University of Freiburg, Germany.

[2]Department of Paediatrics IV, University Children's Hospital Tuebingen, Germany.

[3]Department of Diagnostic Imaging, University Children`s Hospital Zurich, Switzerland.

[4]Children's Research Center, University Children's Hospital Zurich, Switzerland.

[5]University of Zurich, Switzerland.

***Corresponding Author(s): Julia Geiger**

University Children`s Hospital, Eleonore Foundation, Steinwiesstr. 75, 8032 Zürich, Switzerland.

Tel: +41-44-266-3386, Fax +41-44-266-7158;

Email: julia.geiger@kispi.uzh.ch

Received: Apr 01, 2022

Accepted: Apr 25, 2022

Published Online: Apr 27, 2022

Journal: Annals of Cardiology and Vascular Medicine

Publisher: MedDocs Publishers LLC

Online edition: http://meddocsonline.org/

Keywords: 4D Flow MRI; Aortic coarctation; Bicuspid aortic valve; Wall shear stress; Oscillatory shear index.

Abstract

Background: Patients after repair of Aortic Coarctation (CoA) have high risk of secondary vessel pathologies; thus, regular monitoring is absolutely essential.

Objective: To investigate aortic hemodynamics and wall parameters in adolescent patients and young adults after repair of CoA by 4D flow MRI in a longitudinal study.

Materials and methods: Time-resolved flow-sensitive 4D MRI was acquired twice in 28 patients (age t1: 14.6±7.8, t2: 18.9±8.3 years) with a mean follow-up duration of 4.4±1.2 years. Quantitative analysis included segmentation of the aorta using 9 manually-placed planes to calculate regional time-averaged absolute Wall Shear Stress (WSS), Peak Velocities (Vmax), Oscillatory Shear Index (OSI) and aortic diameters. Two independent readers assessed blood flow visualisation depicting helical and vertical flow patterns. For statistical analysis, patients who underwent re-intervention and patients with bicuspid aortic valve (BAV) were evaluated separately.

Results: Quantitative analysis showed an overall decrease in WSS (mean t1: 0.48±0.13 N/m², t2: 0.33±0.11 N/m²; $p<0.005$) and an increase in OSI (t1: 7.16±4.05, t2: 9.98±4.76; $p<0.05$). Peak velocities decreased significantly in the ascending aorta (AAo; t1: 1.42±0.37m/s, t2: 1.27±0.37m/s; $p<0.001$). BAV patients showed lower OSI and higher WSS in the AAo at both examinations, and lower peak velocities in the aortic arch, the CoA site and descending aorta (DAo ($p>0.05$)). The total number of secondary flow patterns decreased except for an increase in additional local AAo helices.

Cite this article: Hirtler D, Romberg J, Stiller B, Geiger J. Longitudinal Evaluation of Aortic Haemodynamics in Patients after Repair of Aortic Coarctation: A 4D Flow MRI Follow-Up Study. Ann Cardiol Vasc Med. 2022; 5(1): 1062.

Conclusion: 4D flow MRI enables us to evaluate qualitative and quantitative aortic changes in patients with repaired CoA over time that are not limited to the CoA site. BAV patients exhibit particular characteristics in quantitative parameters.

Introduction

Aortic Coarctation (CoA) accounts for 4-6% of all congenital heart defects [1]. Although usually occurring in isolation, CoA is frequently associated with bicuspid aortic valve (BAV) [1], valvar aortic stenosis, and ventricular septal defect [2]. There are different etiological hypotheses: residual ductal tissue at the isthmic site of the aorta, or genetic disorders associated with a Vascular Endothelial Growth Factor (VEGF) mutation. Altered aortic-wall composition involving a higher percentage of collagen fibers and fewer smooth muscle cells in the prestenotic segment and a modified fetal blood flow are also discussed [3,4].

Even when treated early in life, the risk of secondary arterial hypertension persists in these patients for up to 10 years after repair, and even without restenosis [5,6]; this is caused by increased left ventricular mass and stiffness combined with arterial stiffness [3]. Aneurysm formation in cerebral arteries [3], in the ascending (AAo) and descending aorta (4-7%) (DAo) associated with BAV or residual stenosis (3-4%) have been reported [7,8]. Age at repair, type of operating procedure, coexisting BAV, aortic geometry, hypoplastic aortic arch and arterial hypertension are several risk factors leading to secondary complications after repair [9-11].

Transthoracic echocardiography is the primary imaging modality for monitoring CoA patients concerning secondary pathologies. However, with increasing age, limitations due to a poor acoustic window might compromise the evaluation of potential re-stenosis or collaterals. MRI is the preferred alternative modality for non-invasive follow-up imaging of CoA, since heart function and aortic anatomy are readily assessable via multiplanar CINE-imaging and MR angiography [12].

4D flow MRI has recently evolved as an advanced technique for the comprehensive assessment of aortic pathologies in terms of haemodynamic alterations in blood flow parameters and flow patterns: Studies in patients with various aortic diseases have shown that abnormal valve opening in BAV patients or stenosis in patients after CoA repair, for example, result in altered flow patterns and Wall Shear Stress (WSS) distribution compared to controls [13-17]. WSS representing frictional forces imposed by the blood flow on the vessel wall, and Oscillatory Shear Index (OSI) expressing the ratio of WSS induced by backward and forward flow are the two main vessel wall parameters examined in this study.

A previous study in adolescents after CoA repair reported a significant increase in overall aortic WSS and a decrease in overall OSI in patients compared to not age-matched healthy volunteers [13]. The same study revealed a higher incidence of additional helical and vortical flow patterns throughout the thoracic aorta including the orifices of the supra-aortic arteries compared with volunteers. This study showed that haemodynamic changes are not limited to the CoA site, but affect the thoracic aorta throughout. However, the role of altered blood flow, WSS and OSI in CoA patients is not yet fully understood because of the lack of long-term follow-up data.

The purpose of our study was to analyze the evolution of aortic haemodynamics during longitudinal follow-up of adolescent patients and young adults after CoA repair by 4D flow MRI in order to obtain deeper insight into the underlying haemodynamic alterations. We hypothesize that increasing abnormal aortic blood flow patterns and alterations in WSS and OSI distribution might occur in patients after CoA repair over time.

Materials and methods

Study cohort

28 paediatric/young adult patients (16 male) were included prospectively and underwent 4D flow MRI of the thoracic aorta at baseline (t1) and follow-up (t2). Patients` demographics are shown in Table 1. Eleven patients were treated for arterial hypertension. 12 patients had undergone an intervention between t1 and t2. 4D flow MRI was added to the standard-of-care cardiothoracic MRI, which was clinically indicated. All patients had routine echocardiography which showed normal left ventricular function at baseline and follow-up. The study was approved by our local ethics board and informed consent was obtained from all participants of the study or their parents.

MR imaging

At follow-up, all patients were scanned on a 1.5T system (Avanto, Siemens, Germany) with a 12-channel body-phased array coil. 15 patients were examined on a 3T MR system (Trio, Siemens, Germany) at baseline examination. 4D flow MRI (k-space segmented rf-spoiled gradient echo sequence with interleaved 3-directional velocity encoding) acquisitions were synchronised to the heart rate and breathing using prospective ECG-gating and adaptive diaphragm navigator gating. 4D flow data were acquired with full 3D coverage of the thoracic aorta and the following sequence parameters: velocity sensitivity = 150-250cm/s, TE=2.4-2.7ms, TR=4.8-5.0ms, FOV=210-270mm x 275-360mm, spatial resolution=(1.7-2.9) x (1.5-2.4) x (2.2-3.5) mm^3, temporal resolution ~ 38-48ms, flip angle 15°.

Parallel imaging (GRAPPA) with a reduction factor of 2 was used. Scan time was about 8-12 minutes depending on the respiratory gating efficiency and heart rate.

Prior to 4D flow acquisitions, all patients underwent time-resolved contrast-enhanced MR angiography (CE-MRA) (0.1mmol/kg gadoteridol; TE=0.9-1.4ms, TR=2.1-3.5ms, spatial resolution=(0.9-1.4) x (0.9-1.4) x (1.2-1.6)mm^3, temporal resolution=2.8-4.2s, FA 11-25°).

Data analysis

4D flow data was postprocessed using home-built software programmed in Matlab (The MathWorks Inc., USA) for noise reduction, velocity anti-aliasing and correction for eddy-current induced phase offset errors [18]. A 3D Phase-Contrast MR Angiogram (PC-MRA) was generated. 3D aortic flow was visualised by time-resolved 3D pathlines and streamlines during the cardiac cycle's different time frames (EnSight 9.2, CEI, Apex, USA). Secondary flow patterns (helices and vortices) in the AAo, aortic arch, proximal and distal the coarctation, in the DAo and supra-aortic arteries were analysed by two independent experienced observers concerning the absence = 0 or presence = 1 of secondary flow patterns. We defined helical flow as a spiral movement along the flow direction axis, and vortical flow as re-circulating areas deviating from the anticipated physiological flow direction. In case of a discrepancy between readers, a third reader was asked to provide a consensus reading.

Quantitative evaluation was based on eight manually-placed analysis planes transecting the aorta orthogonal to the main blood flow direction. An additional analysis plane (plane 9) was placed at the site of repair and/or (re-) coarctation; in eight patients with stent implantation plane 9 was placed directly at the stent's distal end (Figure 1). Using a homebuilt analysis tool based on MatLab (The Mathworks Inc, USA), we quantified blood flow, vessel diameters, and wall parameters. Magnitude and flow data from all nine analysis planes were exported to the analysis tool to manually segment the lumen boundaries in all cardiac phases. Absolute WSS averaged over the cardiac cycle (WSSmag), OSI and peak systolic velocity (Vmax) were calculated for each analysis plane [19].

Diameter measurements

Vessel diameters were delivered as the maximum diameter during the cardiac cycle.

Aortic diameters were compared in four aortic segments: AAo and DAo at level of pulmonal artery, aortic arch and CoA. Relative aortic diameters were calculated in relation to the distal DAo at the diaphragm level as done by Pinzon, Lemler and Bogaert [9,20,21]. According to Bogaert et al, ratios of AAo/DAo ≥1.5 are indicative for dilatation, ≤0.9 for stenosis.

Statistical analysis

Patients were divided into subgroups for statistical analysis: those with an intervention between the baseline and follow-up examination, and patients with no intervention. The non-intervention group was further subdivided in patients with tricuspid (TAV) and bicuspid aortic valve (Table 2/Figure 2).

Quantitative values between baseline and follow-up examinations were compared using a two-sided paired t-test. To compare haemodynamic parameters between different subgroups (intervention vs non-intervention), a non-paired t-test was applied. McNemar test with correction factor of Edwards and Yates was used to analyse flow patterns over time. Interobserver variability for flow visualisation was assessed by Cohen´s Kappa test (Kappa coefficient). All tests applied a significance level of $p<0.05$. Statistics were analysed using SPSS Statistics 22 (IBM Corporation).

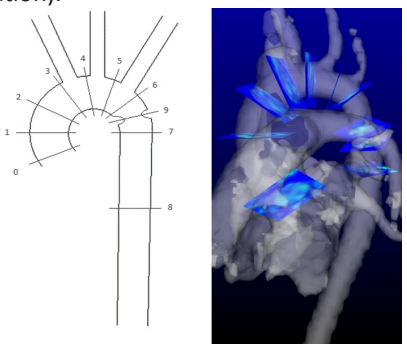

Figure 1: Quantitative evaluation was based on nine manually-placed analysis planes along the thoracic aorta, which are orthogonal to the main blood flow direction. Plane 9 is located at the CoA level. Plane 0 was only used to generate particle traces and streamlines. Left: Schema of the thoracic aorta with position of the planes. Right: Isosurface with manually-placed planes.

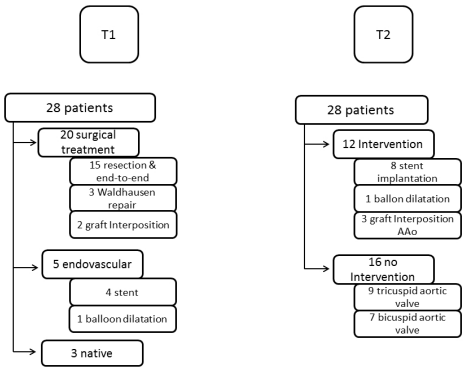

Figure 2: This diagram shows the patient cohort at baseline (t1) and follow-up examination (t2) grouped after type of repair/intervention, non-intervention and aortic valve.

Table 1: Demographics of all patients.

	T1	T2
Age at examination (yr)	14.6 ± 7.8 (4.1-36.8)	18.9 ± 8.3 (6.8 – 43.1)
Gender	12 female, 16 male	
Body weight (kg)	45.9 ± 20.8 (16 –91)	55.6 ± 18.4 (20 – 93.1)
Time interval since repair (yr)	11.3 ± 6.5 (1.3 – 28.9)	15.6 ± 8.8 (1.1 – 39.4)
Time interval between baseline and follow-up examination (yr)	4.35 ± 1.2 (2.1 – 6.4)	
Blood pressure at rest (mmHg) • Systolic • Diastolic	 120.7 ± 21.8 (82 – 190) 67.8 ± 13.9 (45 – 100)	 126.3 ± 25 (85 – 192) 68.2 ± 12.7 (52 – 100)
bicuspid aortic valve	10/28 (+ 1 functional bicuspid)	

Data is given as: Mean ± SD (range)

Table 2: Demographics of different patient subgroups at follow-up examination.

	Patients with intervention (n=12)	Patients without intervention			p-value*
		All (n=16)	TAV (n=9)	BAV (n=7)	
Age at follow up (yr)	20.67 ± 10.1	17.7 ± 6.7	17.6 ± 8.6	17.9 ± 3.7	0.18
Body weight (kg)	58.4 ± 19.2	53.4 ± 18.6	53.6 ± 22.8	53.2 ± 13.2	0.24
Gender (female/male)	4/8	8/8	4/5	4/3	
Blood pressure (mmHg) • Systolic • Diastolic	 131 ± 24 71 ± 16	 123 ± 26 66 ± 10	 134 ± 28 67 ± 9	 109 ± 16 65 ± 11	 0.17 0.91

Patients with and without an intervention between baseline and follow-up examination; Patients without intervention were divided in two subgroups: tricuspid (TAV) and bicuspid (BAV) Aortic Valve. * Intervention vs non-intervention group.

Results

Aortic diameters

Absolute diameters increased at all levels of all patients from t1 to t2: AAo: t1=25.0±6.1mm to t2=28.2±5.4mm, aortic arch: t1=18.3±4.8mm to t2=20.8±3.1mm, CoA: t1=15.5±3.8mm to t2=18.0±3.3mm. However, only absolute DAo diameters increased significantly from t1=17.9±3.8mm to t2=21.3±3.6mm ($p<0.001$).

Relative diameters of all patients decreased significantly at the AAo level (average t1: 1.44±0.29, t2: 1.34±0.18; $p=0.017$). Relative diameters of the aortic arch and CoA did not change significantly.

We made the same findings in the two subgroups (intervention vs. non-intervention): AAo/DAo ratio decreased in both groups, but significantly only in the non-intervention group ($p=0.031$). The intervention group's CoA/DAo ratio increased significantly (t1=0.72±0.16 to t2=0.91±0.12; $p<0.017$). Patients with no re-intervention revealed only a significant increase in the absolute DAo diameter in follow-up ($p<0.001$).

There were no significant differences in aortic diameters between the BAV and TAV patients over time.

Peak systolic velocity

All patients exhibited a significant decrease in Vmax in the AAo (t1: 1.42±0.37m/s, t2: 1.27±0.37m/s; $p<0.001$). No significant changes were observed in the other aortic segments.

BAV patients presented a lower Vmax in all aortic segments than TAV patients, which was significant in the aortic arch ($p=0.005$), at the CoA site ($p=0.031$) and in the DAo ($p=0.007$).

Wall shear stress (WSS)

Time-averaged absolute WSS decreased significantly in all nine planes between t1 and t2 (mean t1: 0.48±0.13 N/m², t2: 0.33±0.11 N/m²; $p<0.005$). Changes were even more pronounced in the non-intervention group ($p<0.002$).

The WSS decrease was independent from the type of aortic valve; patients with BAV had slightly elevated WSS-values in the AAo (planes 1-3) at t1 and t2, however (fig. 3).

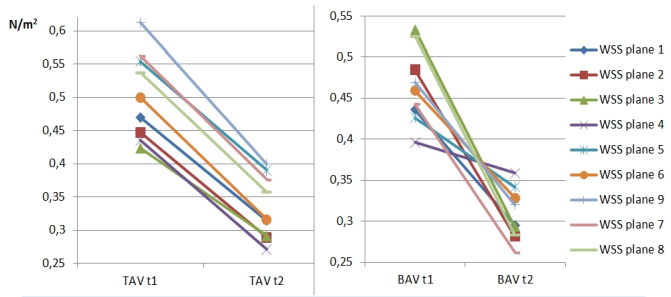

Figure 3: Mean aortic wall shear stress (WSS) at baseline (t1) and follow-up (t2) of the non-intervention group in every plane. BAV: bicuspid aortic valve ($p<0.05$), TAV: tricuspid aortic valve ($p<0.05$).

Oscillatory shear index (OSI)

OSI generally increased in all analysis planes in follow-up (t1: 7.16±4.05, t2: 9.98±4.76; ($p<0.05$ for planes 2-9)). A significant increase was especially obvious in the aortic arch and DAo (planes 3-7; $p=0.015$) in the non-intervention group. Although BAV patients showed a lower OSI than TAV patients at both examinations, the former's observed increase was more pronounced (fig.4).

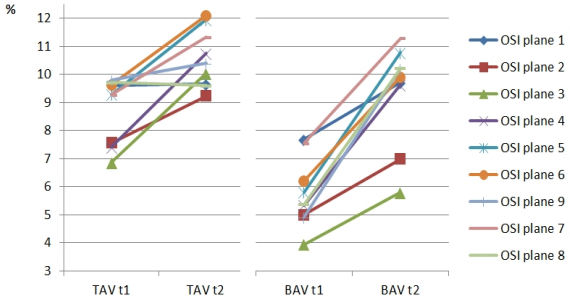

Figure 4: Mean aortic oscillatory shear index (OSI) at baseline (t1) and follow-up (t2) of the non-intervention group in every plane. BAV: bicuspid aortic valve ($p<0.05$), TAV: tricuspid aortic valve ($p<0.05$).

Flow pattern analysis

Interobserver agreement regarding flow visualization was excellent for helical (Cohen's k = 0.77) and vortical flow patterns (Cohen's k = 0.87). Flow pattern analysis was impossible at the CoA site in 8/12 intervention-group patients due to stent artefacts.

We observed a general decrease in vortices in all aortic segments, which was only significant in the AAo ($p<0.05$). Patients with no intervention revealed a significant decrease in vortices at the CoA site ($p<0.05$). Aortic valve morphology did not affect the number of vortices.

Most (26/28) patients presented a physiological right-handed helix in the AAo at t1 and t2. Both groups (intervention/non-intervention) showed a significant increase in additional helices in the AAo ($p<0.05$). The non-intervention group exhibited a significant increase in helices at the left subclavian artery's origin. Moreover, we observed a significant increase in AAo helices in BAV patients (Figures 5 & 6).

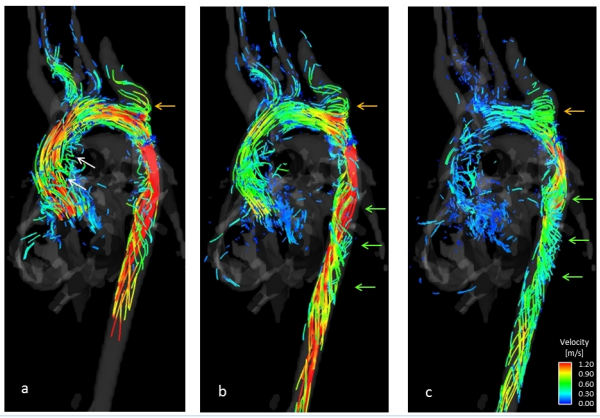

Figure 5: 11 year-old patient, 11 years after surgical end-to-end repair. Small additional helical formation in the ascending aorta (white arrows) in the early systole (a). Additional vortical blood flow in the left subclavian artery (orange arrows) all over the heart cycle (a-c). And distinct helical flow pattern in the descending aorta (green arrows) in the late systole (b) and early diastole (c).

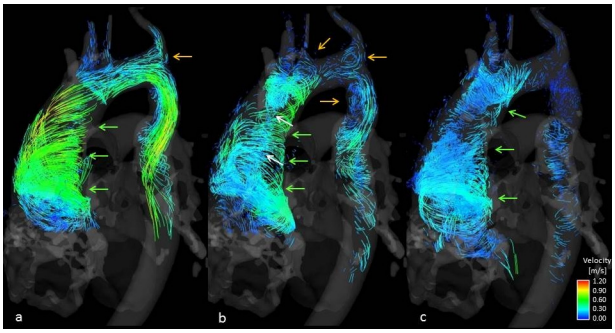

Figure 6: 36 year-old patient with bicuspid aortic valve and tube graft interposition at the coarctation site. Distinct helical blood flow in the dilated ascending aorta (AAo) all over the heart cycle (a-c) (green arrows). Additional helix in the AAo (white arrows) in the late systole (b) and multiple vortices (orange arrows). a: Early systole; c: Early diastole.

Discussion

The results of our 4D flow MRI follow-up study in patients after CoA repair revealed a general WSS decrease and OSI increase throughout the thoracic aorta during a mean follow-up time lasting about four years. Patients with BAV showed distinct haemodynamic parameters, but the same general changes between their baseline and follow-up examination. Our visual assessment of colour-coded pathlines revealed a decrease in the total amount of abnormal flow patterns except for an increase in local AAo helices over time.

A prior study in a CoA patient cohort aged a mean 16.5 years reported a significant increase in overall aortic WSS and a decrease in overall OSI in patients compared to volunteers [13]. That study reported an increased number of local helices and vortices in the thoracic aorta involving the orifices of the supra-aortic branches. An earlier study revealed that WSS is age-dependent with an inverse relationship between age and velocity/WSS [22]. Therefore, age-matching is necessary to assess normal and pathological wall parameters. As the volunteers in the aforementioned study were not age-matched, they had a mean age difference of about 20 years [13].

The changes we noted in our study are therefore difficult to interpret: the WSS decrease could be considered as some sort of (probably transient) normalisation, since those follow-up values were within the range of normal values in healthy subjects provided in the literature [14]. These values are based on a plane-wise approach in eight analysis planes along the thoracic aorta, comparable to our assessment strategy, which included an additional plane at the coarctation level, whereas the age-dependent WSS study took a segmental 3D WSS approach [23]. The plane-wise analysis is more prone to observer-dependent errors due to manual vessel contour segmentation. Reproducible plane placement in follow-up examinations is more difficult than in the more recently introduced 3D WSS calculation that takes advantage of the three-dimensional nature of 4D flow data [22]. This advanced approach to capture 3D WSS was also used in a recent study for assessment of paediatric coarctation [24].

We believe that our study results are most likely a temporary phenomenon, because the growing length during puberty exerts a substantial impact on changes in aortic dimensions and thus haemodynamics.

While previous studies used Z-Scores to assess aortic diameters in children and adolescents in follow-up [25,26], we decided to use AAo/DAo ratios to monitor changes in diameters [9,21]. Since DAo diameters, but not AAo diameters increased significantly during follow-up, our patient group's AAo/DAo ratio decreased. These results were independent from the type of aortic valve or re-intervention during the follow-up period.

Re-interventions are frequently necessary in CoA patients, who are at risk of developing re-stenoses or secondary dilatation at the CoA site or the DAo [2,3]. Patients who have undergone a re-intervention between the baseline and follow-up examination must be evaluated very carefully, because the re-intervention may have an impact not only on the CoA site in terms of diameter, but also on haemodynamics throughout the thoracic aorta [13]. To assess the "natural" course of the disease, however, our evaluation of the patient subgroup that had not experienced a re-intervention is more informative.

There have been very few 4D flow MRI follow-up studies published addressing children and teenagers [25,26]. While the first study investigated young patients with Marfan syndrome aged a mean 14 years at baseline examination over a 3-year period [25], the second study surveyed BAV patients aged a mean 13 years over less than two years [26]. Both studies reported rather stable haemodynamics in each patient group over time. Exceptions were the local changes in the proximal DAo in the Marfan group, and significant AAo growth in BAV patients.

In our study, 7/16 patients in the non-intervention group had a BAV, which is frequently associated with CoA. There are several published studies on BAV patients, mainly adults, which have shown that altered AAo haemodynamics and WSS distribution as the results of abnormal valve opening and aortopathy, already evident in children and teenagers [24,27-30,16,31]. A sub-analysis in the study by Allen et al. in young patients with BAV revealed no differences in velocity and WSS in the AAo between patients with and without CoA; however, patients after repair presented increased velocities and WSS in the aortic arch and DAo [27]. A more recent study in adolescent patients with CoA and BAV also described abnormalities in flow patterns, flow velocities and WSS at several aortic sites that were most pronounced in the transverse arch and descending aorta [24].

Patients with BAV revealed particular haemodynamics in our study. They had higher WSS values in the AAo at both examinations than TAV patients, and decreased concomitant OSI values that were not limited to the AAo. In contrast to another study in adults [32], patients with BAV did not exhibit larger AAo diameters than CoA patients with TAV in our study. However, our patient cohort was considerably younger.

We had anticipated a progression of abnormal flow patterns based on previous studies [13,17]. Nevertheless, the number of abnormal vortices and helices decreased in our study between the first and second examination. Only the local helices in the AAo increased in all subgroups, and interestingly, the helices at the origin of the left subclavian artery in the non-intervention group. Our intervention group's CoA region assessment was compromised by stent-caused artefacts.

Another approach to investigate aortic properties in CoA patients after repair was taken in the study by Schafer et al., who compared aortic elasticity by pulse wave velocity in patients after different types of repair (surgery vs. balloon angioplasty vs. stent) [33]. They found elevated aortic stiffness in the AAo of children after surgery and balloon angioplasty compared to those treated by stent. The presence of BAV augmented the AAo stiffness in their study. In addition, they detected differ-

ences in aortic WSS between their differently-treated coarctation groups. Inconsistencies in the literature regarding elevated or depressed WSS in the AAo in BAV patients can be attributed to varying age groups, BAV types, and assessment strategies, resulting in different ranges of aortic dilatation, disease stages and therefore haemodynamics.

A previous study correlated WSS results in BAV patients after aortic resection with extra-cellular matrix (ECM) regulation: Regions exhibiting increased WSS corresponded with ECM dysregulation and elastic fiber degeneration [34]. These findings implicate valve-related haemodynamics as a contributing factor in the development of aortopathy, i.e. mainly affecting anomalous AAo remodelling in BAV patients.

Our study has several limitations: The main one being our heterogeneous patient cohort of patients who underwent different types of primary treatment (resection with end-to-end anastomosis, graft, endo vascular treatment), patients with and without re-intervention in follow-up, and patients with BAV and TAV. Our small study cohort resulted in even smaller subgroups for analysis based on re-intervention and valve morphology.

Hypertension is a known adverse effect in CoA patients [5,6]. Eleven out of 28 patients in our study were taking antihypertensive medication during their baseline and follow-up examinations, which might have affected aortic growth rates, cardiac output, and aortic haemodynamics. The length growth during puberty and its impact on aortic dimensions and haemodynamics was also mentioned above.

Another limitation of our data analysis strategy has to do with the manual plane segmentation that can lead to user variability and errors in the WSS estimation, as discussed earlier. More recently introduced advanced techniques using 3D WSS assessment or even fully quantitative mapping of aortic velocity and WSS may improve measurement reproducibility and thus, optimized monitoring of aortic hemodynamics in these patients [35].

Conclusion

4D flow MRI enables a comprehensive evaluation of qualitative and quantitative changes over time throughout the aorta in patients who have a repaired CoA. Altered haemodynamic parameters seem to normalise in young adults CoA patients in follow-up; however, these changes may be transient and influenced by various factors, such as concomitant BAV. Longer-term follow-up with larger patient cohorts will be needed to better understand how disease progresses in young adult patients after CoA repair and which patients are at increased risk for adverse cardiovascular events.

Acknowledgement

We thank Ramona Lorenz for contributing ideas to statistical analysis and are grateful for language editing by Carole Cuerten.

References

1. Schwedler G, Lindinger A, Lange PE, Sax U, Olchvary J, et al. Frequency and spectrum of congenital heart defects among live births in Germany: A study of the Competence Network for Congenital Heart Defects. Clin Res Cardiol. 2011; 100: 1111-1117.

2. Schimke A, Majithia A, Baumgartner R, French A, Goldberg D, et al. Intervention and management of congenital left heart obstructive lesions. Curr Treat Options Cardiovasc Med. 2013; 15: 632-645.

3. Kenny D, Hijazi ZM. Coarctation of the aorta: From fetal life to adulthood. Cardiology J. 2011; 18: 487-495.

4. Jashari H, Rydberg A, Ibrahimi P, Bajraktari G, Henein MY. Left ventricular response to pressure afterload in children: aortic stenosis and coarctation: a systematic review of the current evidence. Int J Cardiol. 2015; 178: 203-209.

5. Canniffe C, Ou P, Walsh K, Bonnet D, Celermajer D. Hypertension after repair of aortic coarctation-a systematic review. Int J Cardiol. 2013; 167: 2456-2461.

6. Tanous D, Benson LN, Horlick EM. Coarctation of the aorta: Evaluation and management. Curr Opin Cardiol. 2009; 24: 509-515.

7. Vonder Muhll IF, Sehgal T, Paterson DI. The Adult With Repaired Coarctation: Need for Lifelong Surveillance. Can J Cardiol. 2016; 32: 1038. e1011-1035.

8. Bambul Heck P, Pabst von Ohain J, Kaemmerer H, Ewert P, Hager A. Survival and cardiovascular events after Coarctation-Repair in Long-Term Follow-Up (COAFU): Predictive value of clinical variables. Int J Cardiol. 2017; 228: 347-351.

9. Bogaert J, Gewillig M, Rademakers F, Bosmans H, Verschakelen J, et al. Transverse arch hypoplasia predisposes to aneurysm formation at the repair site after patch angioplasty for coarctation of the aorta. J Am Coll Cardiol. 1995; 26: 521-527.

10. Oliver JM, Gallego P, Gonzalez A, Aroca A, Bret M, et al. Risk factors for aortic complications in adults with coarctation of the aorta. J Am Coll Cardiol. 2004; 44: 1641-1647.

11. Ou P, Celermajer DS, Mousseaux E, Giron A, et al. Vascular remodeling after "successful" repair of coarctation: Impact of aortic arch geometry. J Am Coll Cardiol. 2007; 49: 883-890.

12. Karaosmanoglu AD, Khawaja RD, Onur MR, Kalra MK. CT and MRI of aortic coarctation: pre- and postsurgical findings. AJR Am J Roentgenol. 2015; 204: W224-233.

13. Frydrychowicz A, Markl M, Hirtler D, Harloff A, Schlensak C, et al. Aortic hemodynamics in patients with and without repair of aortic coarctation: In vivo analysis by 4D flow-sensitive magnetic resonance imaging. Invest Radiol. 2011; 46: 317-325.

14. Frydrychowicz A, Stalder AF, Russe MF, Bock J, Bauer S, et al. Three-dimensional analysis of segmental wall shear stress in the aorta by flow-sensitive four-dimensional-MRI. J Magn Reson Imaging. 2009; 30: 77-84.

15 Geiger J, Markl M, Herzer L, Hirtler D, Loeffelbein F, et al. Aortic flow patterns in patients with Marfan syndrome assessed by flow-sensitive four-dimensional MRI. J Magn Reson Med. 2012; 35: 594-600.

16. Hope MD, Meadows AK, Hope TA, Ordovas KG, Reddy GP, et al. Images in cardiovascular medicine. Evaluation of bicuspid aortic valve and aortic coarctation with 4D flow magnetic resonance imaging. Circulation. 2008; 117: 2818-2819.

17. Hope MD, Meadows AK, Hope TA, Ordovas KG, Saloner D, et al. Clinical evaluation of aortic coarctation with 4D flow MR imaging. J Magn Reson Med. 2010; 31: 711-718.

18. Bock J KB, Hennig J, Markl M. Optimized pre-processing of time-resolved 2D and 3D phase contrast MRI data. Proceedings of the 15th Annual Meeting of ISMRM, Berlin, Germany (abstract 3138). 2007.

19. Stalder AF, Russe MF, Frydrychowicz A, Bock J, Hennig J, et al. Quantitative 2D and 3D phase contrast MRI: Optimized analysis of blood flow and vessel wall parameters. Magn Reson Med. 2008; 60: 1218-1231.

20. Lemler MS, Zellers TM, Harris KA, Ramaciotti C. Coarctation index: identification of recurrent coarctation in infants with hypo-

plastic left heart syndrome after the Norwood procedure. Am J Cardiol. 2000; 86: 697-699, A9.

21. Pinzon JL, Burrows PE, Benson LN, Moes CA, Lightfoot NE, et al. Repair of coarctation of the aorta in children: Postoperative morphology. Radiology. 1991; 180: 199-203.

22. van Ooij P, Garcia J, Potters WV, Malaisrie SC, Collins JD, et al. Age-related changes in aortic 3D blood flow velocities and wall shear stress: Implications for the identification of altered hemodynamics in patients with aortic valve disease. J Magn Reson Med. 2016; 43: 1239-1249.

23. van Ooij P, Potters WV, Nederveen AJ, Allen BD, Collins J, et al. A methodology to detect abnormal relative wall shear stress on the full surface of the thoracic aorta using four-dimensional flow MRI. Magn Reson Med. 2015; 73: 1216-1227.

24. Desai L, Stefek H, Berhane H, Robinson J, Rigsby C, Markl M. Four-Dimensional flow Magnetic Resonance Imaging for Assessment of Pediatric Coarctation of the Aorta. J Magn Reson Imaging. 2022; 55: 200-208.

25. Geiger J, Hirtler D, Gottfried K, Rahman O, Bollache E, et al. Longitudinal Evaluation of Aortic Hemodynamics in Marfan Syndrome: New Insights from a 4D Flow Cardiovascular Magnetic Resonance Multi-Year Follow-Up Study. J Cardiovasc Magn Reson. 2017; 19: 33.

26. Rose MJ, Rigsby CK, Berhane H, Bollache E, Jarvis K, et al. 4-D flow MRI aortic 3-D hemodynamics and wall shear stress remain stable over short-term follow-up in pediatric and young adult patients with bicuspid aortic valve. Ped Radiol. 2019; 49: 57-67.

27. Allen BD, van Ooij P, Barker AJ, Carr M, Gabbour M, et al. Thoracic aorta 3D hemodynamics in pediatric and young adult patients with bicuspid aortic valve. J Magn Reson Med. 2015; 42: 954-963.

28. Barker AJ, Markl M, Burk J, Lorenz R, Bock J, et al. Bicuspid aortic valve is associated with altered wall shear stress in the ascending aorta. Circ Cardiovasc Imaging. 2012; 5: 457-466.

29. Bissell MM, Hess AT, Biasiolli L, Glaze SJ, Loudon M, et al. Aortic dilation in bicuspid aortic valve disease: Flow pattern is a major contributor and differs with valve fusion type. Circ Cardiovasc Imaging. 2013; 6: 499-507.

30. Hope MD, Hope TA, Meadows AK, Ordovas KG, Urbania TH, et al. Bicuspid aortic valve: Four-dimensional MR evaluation of ascending aortic systolic flow patterns. Radiology. 2010; 255: 53-61.

31. Mahadevia R, Barker AJ, Schnell S, Entezari P, Kansal P, et al. Bicuspid aortic cusp fusion morphology alters aortic three-dimensional outflow patterns, wall shear stress, and expression of aortopathy. Circulation. 2014; 129: 673-682.

32. Frandsen EL, Burchill LJ, Khan AM, Broberg CS. Ascending aortic size in aortic coarctation depends on aortic valve morphology: Understanding the bicuspid valve phenotype. Int J Cardiol. 2018; 250: 106-109.

33. Schafer M, Morgan GJ, Mitchell MB, Ross M, Barker AJ, et al. Impact of different coarctation therapies on aortic stiffness: Phase-contrast MRI study. Int J Cardiovasc Imaging. 2018; 34: 1459-1469.

34. Guzzardi DG, Barker AJ, van Ooij P, Malaisrie SC, Puthumana JJ, et al. Valve-Related Hemodynamics Mediate Human Bicuspid Aortopathy: Insights from Wall Shear Stress Mapping. J Am Coll Cardiol. 2015; 66: 892-900.

35. van Ooij P, Farag ES, Blanken CPS, Nederveen AJ, Groenink M, et al. Fully quantitative mapping of abnormal aortic velocity and wall shear stress direction in patients with bicuspid aortic valves and repaired coarctation using 4D flow cardiovascular magnetic resonance. J Cardiovasc Magn Reson. 2021; 23: 9.